Structural Engineering and Mechanics, Vol. 32, No. 2 (2009) 337-350
DOI: http://dx.doi.org/10.12989/sem.2009.32.2.337

Behavior and simplified analysis of steel-concrete composite beams subjected to localized blast loading

Guo-Qiang Li†

State Key Laboratory for Disaster Reduction in Civil Engineering, Shanghai, China
College of Civil Engineering, Tongji University, Shanghai, China

Tao-Chun Yang‡

College of Civil Engineering, Tongji University, Shanghai, China

Su-Wen Chen‡†

State Key Laboratory for Disaster Reduction in Civil Engineering, Shanghai, China
College of Civil Engineering, Tongji University, Shanghai, China

(Received March 2, 2009, Accepted April 13, 2009)

Abstract. Finite element simulations are increasingly used in structural analysis and design, especially in cases where complex structural and loading conditions are involved. Due to considerable progresses in computer technology as well as nonlinear finite-element analysis techniques in past years, it has become possible to pursue an accurate analysis of the complex blast-induced structural effects by means of numerical simulations. This paper aims to develop a better understanding of the behavior of steel-concrete composite beams (SCCB) under localized blast loading through a numerical parametric study. A finite element model is set up to simulate the blast-resistant features of SCCB using the transient dynamic analysis software *LS-DYNA*. It is demonstrated that there are three dominant failure modes for SCCB subjected to localized blast loading. The effect of loading position on the behavior of SCCB is also investigated. Finally, a simplified model is proposed for assessing the overall response of SCCB subjected to localized blast loading.

Keywords: SCCB; localized blast loading; finite element model; position of blast loading; failure modes; simplified design method.

1. Introduction

Structural components may be subjected to a wide range of deliberate impulsive loads such as accidental explosions or terrorist bomb attacks. To deal with the extreme structural effects, structural engineers are seeking new methods of assessment, analysis and design for high-risk facilities against

† Professor, E- mail: gqli@tongji.edu.cn
‡ Ph.D. Candidate, Corresponding author, E-mail: yangtaochun@hotmail.com
‡† Associate Professor, E-mail: swchen@tongji.edu.cn

shock and blast loads. A number of researchers have undertaken experimental and numerical studies on steel or RC beams subjected to blast loading. Krauthammer put forward a single-degree-of-freedom (SDOF) method, which could be effectively employed to evaluate structural member performances, and conducted research on the dynamic response and failure mode of RC beams under blast loading based on the theory of Timoshenko beam (Krauthammer 1984, Krauthammer *et al.* 1986). With a modal analysis approach Ross (1983) conducted a research on elastic Timoshenko beam under blast loading, taking the rotary inertia and shear deformation into account, and demonstrated that a shear failure could occur before a bending failure in such beams. Ghabossi et al (1984) used a numerical method to analyze the results of FOAMHEST experiment. In more recent years, Izzuddin and Fang analyzed the constitutional relationship and dynamic performance of steel material subjected to blast loading (Izzuddin *et al.* 1997, Fang *et al.* 1997). Liew and Chen studied the dynamic responses of steel beam and column with different kinds of elements (Liew *et al.* 2004, Chen *et al.* 2005). Song and Izzuddin investigated the dynamic response of steel frames under blast loading using a non-linear analysis method (Song *et al.* 2000, Izzuddin *et al.* 2000).

While a large number of finite element models have been developed and utilized to simulate the behavior of steel and RC beams, little has been done on the analysis of steel reinforced composite beams (SCCB) or similar components under blast loading.

SCCB can bear tremendous structural loads; they are used often to protect buildings against extreme loading conditions such as earthquakes. However, the behavior of SCCB subjected to blast effects is not clearly known. To fill in this gap, a numerical parametric study has been conducted to investigate into the behavior of SCCB under localized blast loading. Due to the involvement of complex interactions between the steel and concrete in SCCB type of components, a non-linear finite element model is deemed to best suit the purpose of the analysis. Using an appropriate FE model allows for a detailed observation on the nonlinear response and the development of failure modes.

The results of such an analysis are expected to provide good insights into the characteristics of SCCB subjected to blast loading. The research programme and the main results are reported in this paper.

2. Blast loading

When a high explosive (HE) charge is detonated, detonation waves will be generated and then propagate in the charge, leading to a sudden release of the explosive energy. For a contact or close-in explosion, a localized blast load on the medium will be produced due to the reaction of the contact / reflection surface to the blast waves.

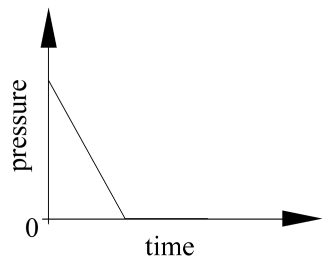

Fig. 1 Simplified pressure history

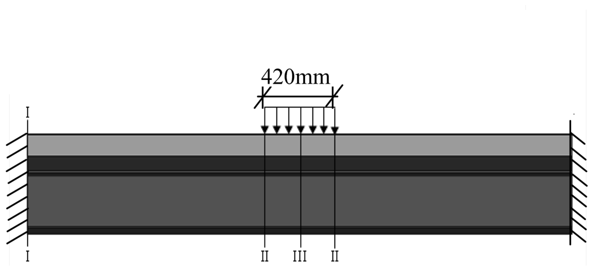

Fig. 2 SCCB under localized blast loading

In general, blast loading is highly impulsive, exhibiting high-pressures that last for a very short duration. In practical engineering analysis, blast loading is frequently simplified into a triangular pulse with a peak pressure and a short duration, as shown in Fig. 1 (Henrych 1979). The localized blast loading imposed on a SCCB may be simplified as uniformly distributed over a limited area, as illustrated in Fig. 2.

3. Finite element model

The configuration of a typical SCCB is shown in Fig. 3. The span of the SCCB is 3000 mm. The thickness and width of the flange of the steel beam for the SCCB is 12 mm and 200 mm respectively. The web plate is designed as 300 mm in height and 8 mm in thickness. The steel beam is modeled using 4600 solid elements with six degrees of freedom at each node. The concrete slab is modeled using 40500 solid elements. Steel reinforcing bars in the concrete slab are modeled by 820 two-node bar elements. The SCCB is assumed to be fully fixed at both ends.

4. Material models

LS-DYNA (2007) software includes a library of nonlinear elastic-plastic material models. In the present analysis, the material model for isotropic and kinematic hardening plasticity considering rate effects is used for steel. Strain rate is accounted for using the Cowper and Symonds model which scales the yield stress with a stress magnification factor as

$$\gamma = 1 + \left(\frac{\dot{\varepsilon}}{C}\right)^{1/p} \tag{1}$$

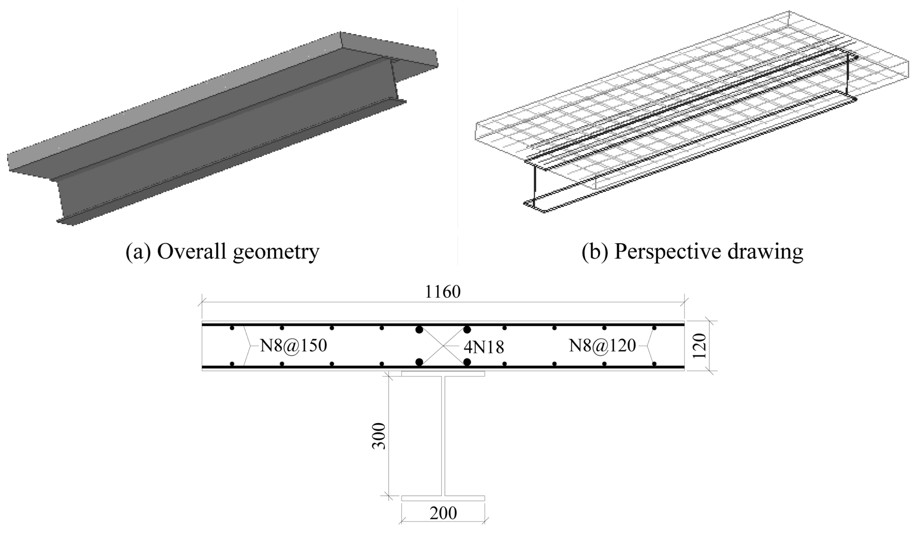

(a) Overall geometry (b) Perspective drawing

(c) Reinforcement drawing

Fig. 3 Configuration of SCCB

Table 1 Steel properties

Young's modulus EX	Poisson's ratio ν	Mass density ρ	Yield stress σ_y	Tangent modulus ETAN	Hardening parameter β	Strain rate parameter C	Strain rate parameter P
206	0.27	7.85	0.31	3.09	0	40	5

Note: The units for the parameters are g for density, cm for length and μs for time.

where $\dot{\varepsilon}$ is the strain rate; P and C are strain rate parameters (Hallquist 1988). The basic steel properties used for the analysis are given in Table 1.

HJC model (Hallquist 1988) is used for concrete material. This model takes large strain, high strain rate and high pressure into account. A normalized equivalent stress is defined as

$$\sigma^* = \frac{\sigma}{f_c'} \tag{2}$$

where σ is the actual equivalent stress, and f_c' is the quasi-static uniaxial compressive strength. The strength surface is expressed as

$$\sigma^* = [A(1-D)+BP^{*N}](1+C\ln\dot{\varepsilon}^*) \tag{3}$$

where A is the normalized cohesive strength, B is the normalized pressure hardening, C is the strain rate coefficient, N is the pressure hardening exponent, D is the damage parameter, P^* is the normalized pressure and $\dot{\varepsilon}^*$ is the dimensionless strain rate. The model's accumulated damage is expressed as

$$D = \sum \frac{\Delta\varepsilon_P + \Delta\mu_P}{D_1(P^*+T^*)^{D_2}} \tag{4}$$

where D_1 and D_2 are damage constants, $\Delta\varepsilon_P$ and $\Delta\mu_P$ are the equivalent plastic strain and plastic volumetric strain and T^* is the normalized maximum tensile hydrostatic pressure.

The pressure for fully dense material is expressed as

$$P = K_1\bar{\mu} + K_2\bar{\mu}^2 + K_3\bar{\mu}^3 \tag{5}$$

where K_1, K_3 and K_3 are material constants and $\bar{\mu}$ is the modified volumetric strain.

Table 2 Concrete material parameters for model

ρ	f_c'	A	B	C	SF_{max}	G	D1	D2	N
2.4	4.8×10^{-4}	0.79	1.60	0.007	7.0	0.1486	0.04	1.0	0.61
EF_{min}	T	P_c	μ_c	P_{lock}	μ_{lock}	K1	K2	K3	EP
0.01	4×10^{-5}	1.6×10^{-4}	0.001	0.008	0.1	0.85	−1.71	2.08	34.5

Note: The units for the parameters are g for density, cm for length and μs for time. ρ and G are mass density and shear modulus, T is maximum tensile hydrostatic pressure, SF_{max} and EF_{min} are normalized maximum strength and amount of plastic strain before fracture, P_c and μ_c are crushing pressure and crushing volumetric strain, P_{lock} and μ_{lock} are locking pressure and locking volumetric strain. The physical meanings of other parameters are described in the introduction of HJC mode.

The relevant parameters for the concrete material model are shown in Table 2. The maximum allowable plastic strain is defined as 0.01, which means that an element is considered to have reached failure, and hence will be deleted, when the maximum plastic strain exceeds 0.01.

It should be mentioned that the relative slip between the concrete slab and steel beam is small because of the action of shear connector in a real SCCB, and the effect of a small slip on the behaviour of a SCCB under localized blast loading is insignificant (Yang 2008). For these reasons, the slip between the concrete slab and the steel beam is ignored in the present analysis; in other words, the concrete slab and steel beam is assumed to work together perfectly.

5. Effects of blast loading position

A localized explosion may occur at any position of the SCCB. To have a better understanding of the effects of the localized blast loading on the behavior of SCCB, three different loading positions are investigated, as shown in Fig. 4. The over-pressure and duration of the blast loading are 1.0 GPa and 0.1 ms respectively. This load case can be produced by a charge weight of 1.5 kg (TNT equivalent) with a standoff distance of 0.3 m approximately.

The deformation of the SCCB subjected to the localized blast loading is shown in Fig. 5. It can be observed clearly that much larger deformation appears in the SCCB within the loading zone than

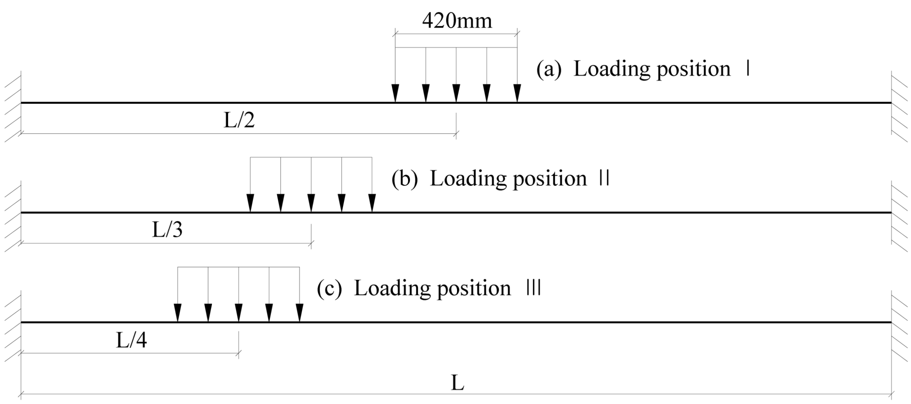

Fig. 4 Different positions of the localized blast loading

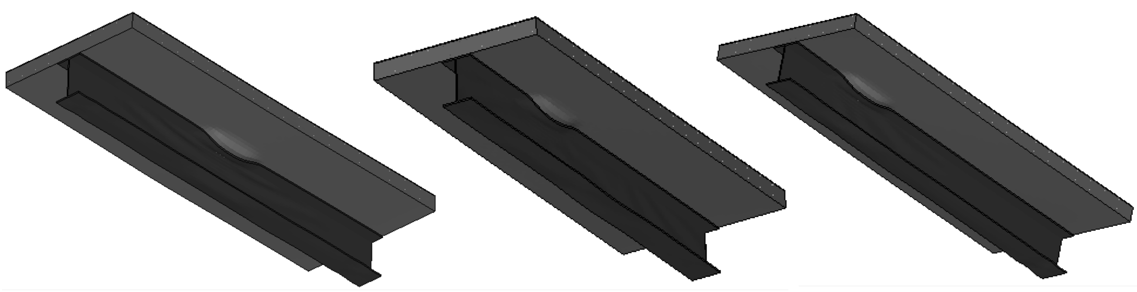

(a) Loading position I (b) Loading position II (c) Loading position III

Fig. 5 Deformation profiles of SCCB under different loading positions

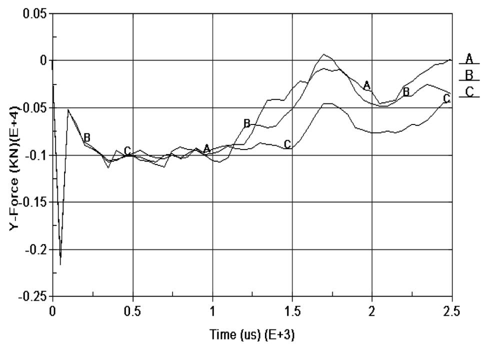

(a) Shear force history at section II

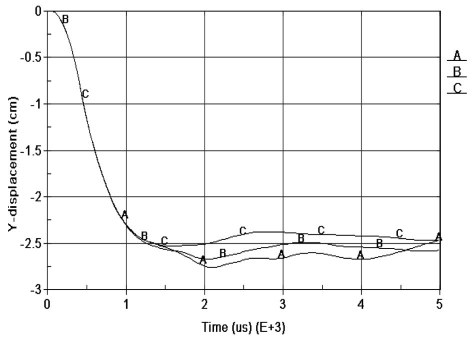

(b) Deformation history at mid-span

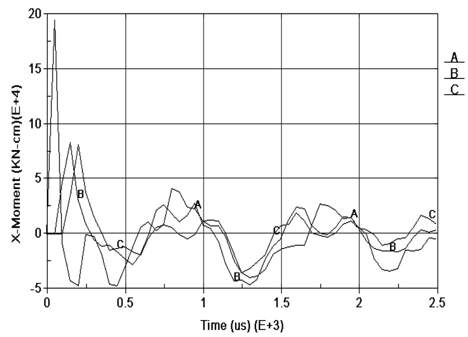

(c) Moment history at mid-span

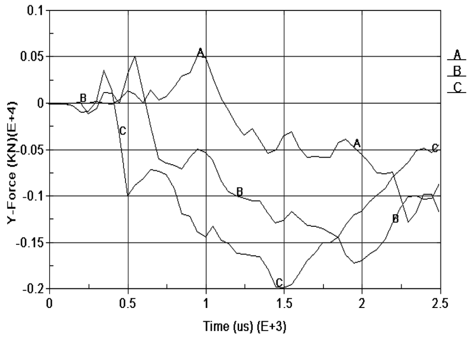

(d) Shear force history at support

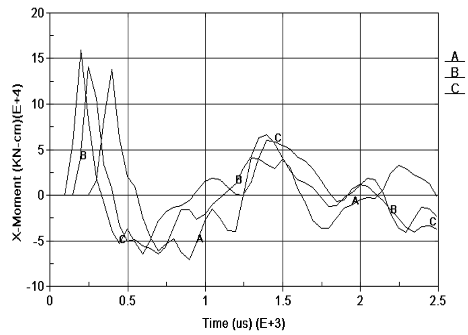

(e) Moment history at support

Note: A - loading at position I, B - loading at position II, C - loading at position III

Fig. 6 Shear force and moment history in the SCCB

that over the remaining region. Although the whole beam continues to deform due to the kinetic energy gained from the blast impulse, the energy imparted to the SCCB is mainly absorbed by the much larger local deformation as compared to the small global deformation of the SCCB during the direct blast loading.

The shear force and moment at a number of sections of the SCCB under three different loading positions are obtained and compared in Fig. 6. It can be observed that there is no big difference in the shear force at the section II of the SCCB under different loading positions. The shear force histories before 0.5 ms and the maximum shear forces at section II are nearly equal. The same is true for the vertical deformation history at mid-span before 0.5 ms. However, the maximum vertical deformations at mid-span are noticeably different. When the localized blast loading acts at the mid-span, the vertical deformation at mid-span has the biggest value. The moment at the mid-span section is also affected by the loading positions significantly. The mid-span section moment is the largest when the blast loading zone is located at the mid-span. It is also found that the maximum shear force and moment at the support of the SCCB change with the variation of loading position. The closer the loading position is to the support, the greater the shear and moment values are.

6. Failure modes

The failure modes are not only related with the impulse, but also affected by the peak pressure and duration of localized blast loading. Further analysis is investigated through changing the impulse, over-pressure and duration respectively. The results indicate that there are three major failure modes for SCCB subjected to localized blast loading. Firstly, when the impulse is very small but the over-pressure is high, only a small area of concrete in the SCCB will be damaged because the impulse is not high enough to result in overall damage. The damage pattern of this case is

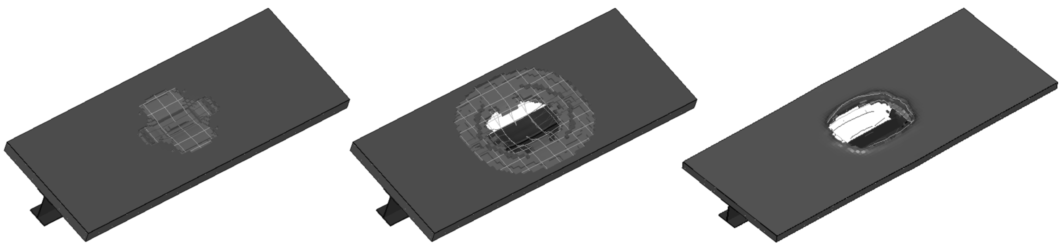

(a) Minor concrete damage (b) sever concrete damage (c) Punching shear damage

Fig. 7 Damage modes of SCCB under different impulses and over-pressures

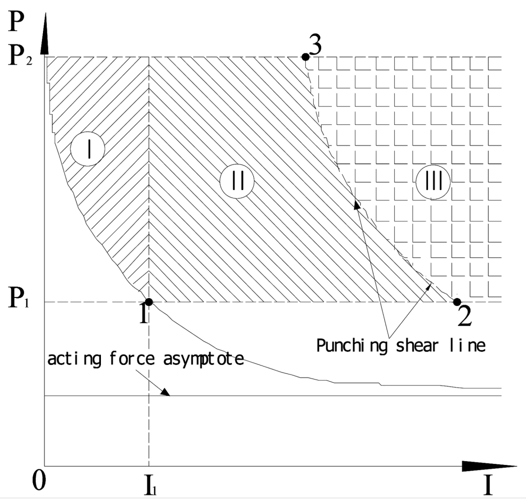

Fig. 8 Pressure-impulse diagram for failure modes of SCCB

shown in Fig. 7(a). Secondly, if the impulse and over-pressure are both high, the concrete near the blast loading zone will be damaged completely, while local bending deformation also occurs in the steel beam. The damage pattern of this case is shown in Fig. 7(b). Thirdly, local punching shear failure will appear if both the impulse and over-pressure are increased further, which is illustrated in Fig. 7(c).

The three different damage modes of SCCB, shown in Fig. 7 may be evaluated with a pressure-impulse diagram as shown in Fig. 8. There are typically three zones corresponding to different failure modes in the pressure-impulse diagram. Zone I has small impulse but high over-pressure, corresponding to the local concrete damage failure mode as shown in Fig. 7(a). Zone II is under the direct effect of shock wave, corresponding to flexural failure mode as shown in Fig. 7(b). In this case, local large deformation in steel beam at mid-span of the composite beam will be generated because of the damage of concrete. Zone III corresponds to punching shear failure mode, which is a kind of brittle failure as shown in Fig. 7(c).

To have a better understanding of the failure modes of SCCB subjected to localized blast loading, the moment and deformation histories at mid-span of the composite beam under the three different blast loadings are examined, as shown in Figs. 9-11. It can be observed that when the over-pressure is small (P=1 GPa, Fig. 9), the moment value and the vertical deformation are small and the moment decreases with the decaying vibration. This indicates that, although the concrete in the slab for the composite beam is damaged, the bearing capacity of SCCB degrades slightly. Such a case can be classified as local concrete damage failure. With increased impulse and over-pressure (P=5 GPa, Fig. 10), the moment and the vertical deformation at mid-span both become relatively larger. After the blast pulse reduces to zero, the moment in the beam drops sharply; however, relatively large permanent deformation remained in the composite beam because of the development of yielding in the steel beam. This features a flexural failure. A punching shear failure occurs under extreme impulse and over-pressure (P=10 GPa, Fig. 11). In such a case, the concrete segment at mid-span will break away, giving rise to a flying debris as indicated in the displacement history shown in Fig. 11.

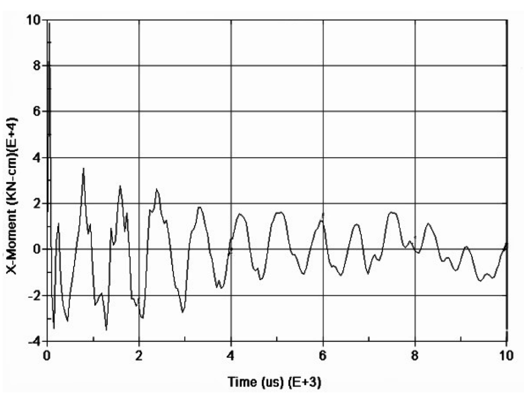

(a) Moment history at mid-span

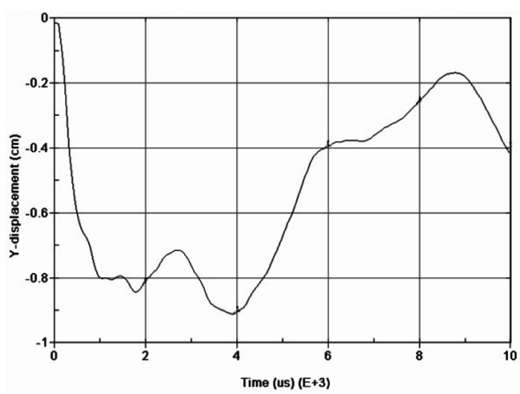

(b) Y-displacement history at mid-span

(P=1GPa, t=0.05ms: equivalent to approximately 0.5kg TNT at standoff distance of 0.2m)

Fig. 9 Moment and Y-displacement history of the SCCB

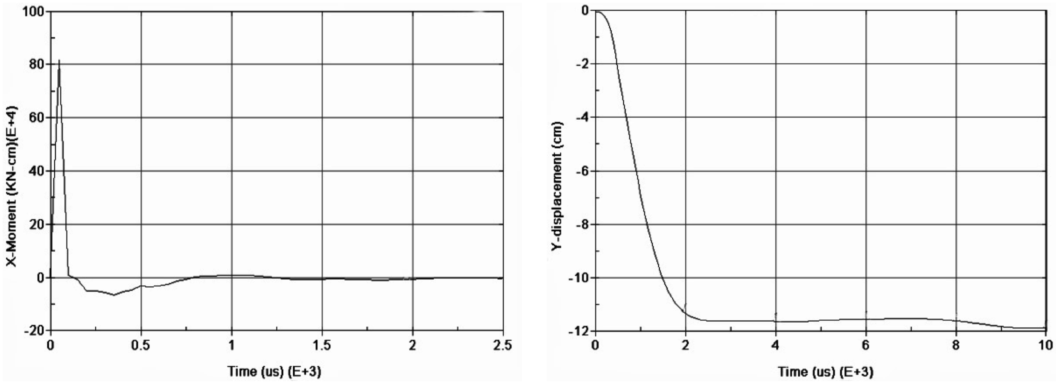

(a) Moment history at mid-span (b) Y-displacement history at mid-span

(P=5GPa, t=0.05ms: equivalent approximately to 1.5kg TNT at standoff distance of 0.1m)

Fig. 10 Moment and Y-displacement history of SCCB

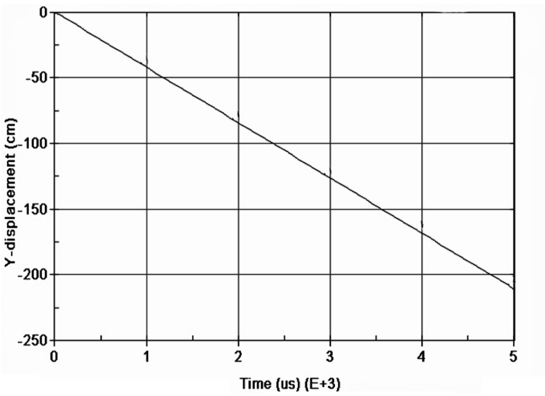

(P=10GPa, t=0.05ms: equivalent approximately to 3.5kg TNT at standoff distance of 0.1m)

Fig. 11 Y-displacement history at mid-span of the steel beam

7. Simplified method for design analysis

As discussed in Section 6, different local failure patterns may be produced in a SCCB under localized blast loading. A classification of the localized failure modes may be made by means of a P-I diagram. As far as the overall structural effect is concerned, however, the mid-span deformation is deemed to be a good indicator of the structural response, and therefore may be considered to relate to the structural design requirements of the SCCB. In this section, a single-degree-of-freedom (SDOF) approach is proposed for an estimation of the global (mid-span) displacement for the structural design of SCCB subjected to blast loading.

Considering that the global deformation of SCCB subjected to localized blast loading is very small during the blast, and ignoring the localized energy absorption (a conservative treatment concerning the overall deformation), it may be assumed that the blast impulse is completely transformed into the initial kinetic energy of the SCCB. Then the kinetic energy will be converted

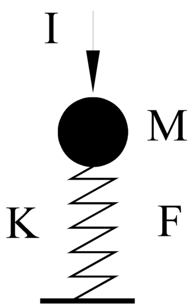

Fig. 12 Single-degree-of-freedom model

into strain energy stored in the SCCB when the maximum deformation is reached. For an estimation of the overall deformation, the SCCB can be modeled as a single-degree of freedom system, as shown in Fig. 12.

According to the general impulse and energy principle, the initial kinetic energy of the SDOF system is given as

$$E_k = \left(\frac{M}{2}\right)\left(\frac{I}{M}\right)^2 = \frac{I^2}{2M} \tag{6}$$

where, $E_k = E$, E = total energy of the system; M = equivalent mass of the system; and I = impulse of localized blast loading.

During the dynamic response of the system subjected to the impulse of blast loading, the kinetic and strain energy will be converted to each other. The total energy can be calculated by the following equation

$$E = \int_V \left(\rho w^{\text{int}} + \frac{1}{2}\rho \upsilon_i \upsilon_i\right) dv \tag{7}$$

where ρ = mass density; w^{int} = energy of unit mass; υ_i = velocity of unit mass; V = volume of object.

According to energy conservation theory, the kinetic energy will convert into potential energy of SDOF when the maximum deformation is reached. In general, the total potential energy consists of elastic potential energy and plastic strain energy, and in a SDOF system this can be expressed as

$$E_p = \frac{1}{2}K \cdot Y_1^2 + F \cdot Y_2 \tag{8}$$

where, $E_p = E_k = E$; K = equivalent elastic stiffness of SDOF; F = force acting on the SDOF system when it is in plastic state; Y_1 = elastic deformation of the system; and Y_2 = plastic deformation of the system.

For the explosion problems of this study, the elastic deformation of SCCB may be neglected because it is relatively small as compared to the plastic deformation. Then the structural material may be regarded as rigid-plastic for a practical analysis of structural response under blast loading. Supposing that the total deformation of the system is Y, and ignoring the elastic deformation, Eq. (8) is simplified to

$$E_p = F \cdot Y \tag{9}$$

Combining Eq. (6) and Eq. (9) yields

$$\frac{I^2}{2M} = F \cdot Y \tag{10}$$

or

$$\frac{I^2}{Y} = 2M \cdot F \tag{11}$$

Introducing a parameter $\omega = 2M \cdot F$, Eq. (11) can be re-written as

$$I^2 = \omega \cdot Y \tag{12}$$

Thus, the relationship between the impulse on a SDOF and the maximum deformation induced is determined by the parameter ω.

The parameter ω is proportional to the product of the effective mass and the generalized yield strength of the system; the effectively mass in turn depends on the deformation profile of the SCCB, which further depends on the beam properties as well as the blast loading. Therefore, the determination of ω is rather complicated. Here we adopt an empirical approach to establish a general understanding of the trend of ω by means of a numerical parametric analysis. Five loading cases, CASE1~CASE5 as listed in Table 3, are investigated on the SCCB shown in Fig. 3. Based on the results in Section 5, the localized blast loading acting at the mid-span is considered the worse scenario concerning the overall displacement; therefore the location of the localized loading is selected at the mid-span in all the five cases. For a blast loading impulse of 4200 N·s, the results of the relevant parameters of the equivalent SDOF system and the dynamic response are summarized in Table 4. Similar investigations are also conducted when the total impulse is 8400 N·s, and the loading cases and analysis results are shown in Table 5 and Table 6 respectively.

Table 3 Loading cases (I = 4200 N·s)

Loading cases	CASE1	CASE2	CASE3	CASE4	CASE5
Pressure (GPa)	5	4	3	2	1
Duration (μs)	20	25	33	50	100

Table 4 Analysis results of SCCB under different loading cases (I = 4200 N·s)

Loading cases	Total energy E (10^5J)	Maximum deformation Y (mm)	Equivalent mass M (Kg)	Equivalent plastic force F (10^6N)	Parameter ω (10^8kg·N)
CASE1	13.66	33	6.5	41.39	5.35
CASE2	12.10	33.5	7.3	36.12	5.27
CASE3	10.37	32.5	8.5	31.91	5.43
CASE4	8.26	33	10.7	25.03	5.35
CASE5	4.79	32	18.4	14.97	5.51

Table 5 Loading cases (I = 8400 N·s)

Loading cases	CASE6	CASE7	CASE8	CASE9	CASE10
Pressure (GPa)	10	5	2	1	0.5
Duration (μs)	20	40	100	200	400

Table 6 Analysis results of SCCB under different loading cases (I = 8400 N·s)

Loading cases	Total energy E (10^5J)	Maximum deformation Y (mm)	Equivalent mass M (Kg)	Equivalent plastic force F (10^6 N)	Parameter ω (10^8 kg·N)
CASE6	42.81	101.5	8.2	42.18	6.95
CASE7	29.48	100	12.0	29.48	7.06
CASE8	18.71	96.5	18.9	19.39	7.31
CASE9	11.35	95	31.1	11.95	7.43
CASE10	6.45	85.5	54.7	7.54	8.25

In general, the maximum deformation in the SCCB varies under different combinations of the over-pressure and duration, even if the total impulse remains the same. However, when the impulse and over-pressure are large enough while the duration is short enough, the maximum deformation of the SDOF system will mainly depend on the blast impulse (Baker *et al*. 1983). The localized blast loading generated by a contact or close-in detonation belongs to this category. This is confirmed by the fact that the maximum deformations for the SCCB are almost the same for blast loads of the same impulse, as can be seen in Table 4 and Table 6, respectively. However, from the FE analysis the total (kinetic) energy of the SCCB decreases with decrease of the over-pressure and increase of the blast duration. Consequently, the effective mass of the equivalent SDOF system should increase (Eq. (6)), whereas the equivalent force applied on the system should decrease (Eq. (9)). The results of the equivalent mass and force listed in Table 4 and Table 6 reflect the above trend. According to Eq. (12), parameter ω will be a constant under a given impulse if Y only depends on the impulse.

The relationship between ω and the SCCB properties can then be obtained by parametric studies and numerical fitting through altering the impulse and the dimensions of SCCB. The following expression is obtained

$$\omega = \frac{(0.0006I+2.65)(46h_c+0.35)(12.65h+1.80)(499t_w+1.96)(144t_f+4.14)}{5.87^4} \tag{13}$$

where, h_c = concrete slab thickness; h = steel beam height; t_w = steel beam web thickness; and t_f= steel beam flange thickness. The unit of ω in Eq. (13) is 10^8 kg·N, the unit of I is N·s, the unit of h_c, h, t_w,and t_f is m.

To check the accuracy of Eq. (13), comparison is made in Table 7 on the values of ω obtained respectively by numerical analysis through using FEM and Eq. (13). It can be observed that Eq. (13) can give a satisfactory prediction of ω.

With Eq. (12) and Eq. (13), the maximum deformation of SCCB subjected to localized blast loading can be easily predicted. Such a prediction may be used for the structural design of SCCB against localized blast loading.

Table 7 Comparison on results of ω

I (N·s)	h_c (mm)	h (mm)	t_w (mm)	t_f (mm)	Numerical analysis (10^8kg·N)	Eq. Ω (10^8kg·N)	Relative error between w_1 and w_2
5250	105	324	8	6	4.59	4.45	3%
5250	120	324	10	10	6.72	6.56	2%
5250	135	324	12	10	8.61	8.38	3%
5250	120	294	6	6	3.88	3.92	8%
5250	120	324	8	10	5.63	5.62	0%
5250	120	339	10	12	7.25	7.12	0%
4200	120	324	8	12	5.35	4.93	8%
5250	120	324	8	12	5.86	5.53	6%
8400	135	339	8	12	8.82	8.19	7%

8. Conclusions

A numerical study using finite element analysis is conducted to investigate the behavior of SCCB subjected to localized blast loading. Results from the study demonstrate that the response of SCCB under localized blast loading is very different from that under conventional loading. The position of localized blast loading has a significant effect on the moment and shear forces at the supports of a SCCB. However, the maximum moment, shear force and deformation over the whole beam vary slightly. It is found that under a localized blast load SCCB fails mainly in three failure modes, namely, local concrete damage, flexural failure and punching shear failure. Punching shear failure, which is a brittle failure mode, should be avoided in the design of SCCB against localized blast loading. Based on the parametric studies through the finite element approach, a simplified method using equivalent SDOF system is proposed for predicting the maximum deformation of SCCB subjected to localized blast loading.

References

Baker, W.E., Cox, P.A., Westine, P.S., Kulesz, J.J. and Strehlow, R.A. (1983), “Explosion hazards and evaluation”, Elsevier Scientific.

Chen, H. and Liew, J.Y.R. (2005), “Explosion and fire analysis of steel frames using mixed element approach”, *J. Eng. Mech.*, ASCE, **131**(6), 606-616.

Fang, Q. and Izzuddin, B.A. (1997), “Rate-sensitive analysis of framed structures. Part II: Implementation and application to steel and R/C frames”, *Struct. Eng. Mech.*, **5**(3), 239-256.

Ghabossi, J., Millavec, W.A. and Isenberg, J. (1984), “R/C structures under impulsive loading”, *J. Struct. Eng.*, **110**(3), 505-552.

Hallquist, J.Q. (1988), *LS-DYNA Theoretical Manual*, Livermore Software Technology Corporation, Livermore.

Henrych, J. (1979), *The Dynamics of Explosion and Its Use*, Elsevier Scientific Publishing Company.

Izzuddin, B.A. and Fang, Q. (1997), “Rate-sensitive analysis of framed structures. Part I: Model formulation and verification”, *Struct. Eng. Mech.*, **5**(3), 221-237.

Izzuddin, B.A., Song, L. and Elnashai, A.S. (2000), “Integrated adaptive environment for fire and explosion analysis of steel frames. Part II: Verification and application”, *J. Constr. Steel Res.*, **53**(1), 87-111.

Krauthammer, T. (1984), “Shallow-buried RC box-type structures”, *J. Struct. Eng.*, **110**(3), 637-651.

Krauthammer, T., Bazeos, N. and Holmquist, T.J. (1986), “Modified SDOF analysis of RC box-type structures”,

J. Struct. Eng., **112**(4), 726-744.
Liwe, J.Y.R. and Chen, H. (2004), “Explosion and fire analysis of steel frames using fiber element approach”, *J. Eng. Mech.*, ASCE, **130**(7), 991-1000.
LS-DYNA Keyword User’s Manual, version 971. Livermore Software Technology Corporation, May 2007.
Ross, T.J. (1983), “Direct shear failure in reinforced concrete beams under impulsive loading”, AFWL-TR-83-84, Kirtland Air Force BASE, NM: Air Force Weapons Laboratory
Song, L., Izzuddin, B.A. and Elnashai, A.S. (2000), “Integrated adaptive environment for fire and explosion analysis of steel frames. Part I: Analytical models”, *J. Constr. Steel Res.*, **53**(1), 63-85.
Yang, T. (2008), “Research on the characteristics of steel-concrete composite beam under contact detonation”, Master Degree Thesis of Tongji University, Shanghai, China.